

Research on Intelligent Simulation Calculation of Interface Connection between Steel and Concrete Composite Beams Based on Discrete Element Method

Yanqiu Ma^{1,a,*}, Jiayuan Chen^{1,b}, Yukang Zeng^{2,c}

¹College of Science and Technology, Hubei University of Arts and Sciences, Xiangyang, 441000, Hubei, China

²Xiangyang Hanxin Sand and Gravel Co., Ltd, Xiangyang, 441000, Hubei, China

^ayanqiuma88@163.com, ^b3421750698@qq.com, ^c2397836225@qq.com

*Corresponding author

Abstract: Steel-concrete composite beams (CB) are widely used in super high-rise buildings, extra-large bridges, underground space engineering and large-scale energy facilities because of their strong bearing capacity, good plastic deformation, convenient construction and low cost. As a result, maintaining the mechanical qualities of steel and concrete constructions requires the integrity of the contact between the two materials. The interface flaws would lessen the steel tube's constraint on the structure's core concrete and alter its mechanical characteristics. Therefore, an essential problem is the intelligent simulation of the interface connection between steel and concrete CB. The goal of this work was to examine the benefits of steel and concrete CB and to model them effectively using the discrete element approach. This work proposed a particle model based on the discrete element approach. The model can effectively establish and analyze the three-dimensional space of buildings in real life, and improve the efficiency of building construction. According to the test results, the maximum durability of rigid joints exceeded 90%, while the maximum durability of spliced steel main beams was only about 70%. Obviously, the elasticity of the rigid joint is higher than that of the spliced steel girder, and the stability was also higher than that of the spliced steel girder. Based on the results of the discrete element method, steel-concrete CB with rigid joints have high stability and elasticity, and can be safely used in different buildings.

Keywords: Steel and Concrete, Discrete Element Method, Smart Simulation, Building Materials

1. Introduction

Composite steel-concrete beams offer several advantages over reinforced concrete beams, including reduced weight, seismic activity and cross-section. It can also increased available space, reduced need for formwork, faster construction time, and increased beam flexibility, it can use less steel. Steel-concrete CB are widely used in large-scale civil engineering structures due to their high bearing capacity, good plastic toughness, superior seismic performance, and convenient construction. As the height of the structure continues to increase, the cross-section of the steel and concrete members also increases. Due to the construction of steel and concrete structures, the steel pipe is generally adjusted and installed in place, and then concrete is poured inside the steel pipe and vibrated for compaction. During the setting process of concrete, hydration heat is generated, The interface between the steel tube and concrete can be damaged by deflection. In steel and concrete structures, the interfacial integrity between the steel tube wall and concrete is an important factor in applying its mechanical properties.

The combined use of steel pipe and concrete can make the composite girder bridge have good mechanical performance and service performance. During the construction of the composite girder bridge, steel beams or trusses can be used to save scaffolding, formwork and high-altitude formwork support procedures, without interrupting the lower traffic, and reducing the amount of on-site construction work. A new type of structure, following steel and concrete, it is the steel-concrete composite beam. High bearing capacity, high rigidity and ductility, good seismic performance, low cost, and simple construction are some of its benefits. It is extensively utilized in structures, highway bridges, and railroad bridges. Shear connectors in CB are crucial to how well they work. Flexible connectors and rigid connectors can be distinguished based on the stiffness classification. It is vital to perform simulation calculations in advance to make sure that the steel beam and concrete can function

well in coordination. The use of the discrete element method to simulate the link between steel and concrete CB is novel in this work.

2. Related Work

Steel-concrete CB are increasingly used in engineering construction due to their many advantages. Its inherent vibration characteristics and dynamic characteristics under coordinated loads have attracted great attention from scientists. To ensure the sustainability of new generation structures, Karthik S. concentrated his study on the utilization of nontraditional building materials. Bamboo strips were employed as concrete pipes in the study, which also included other cement-related materials. These results proved bamboo's durability and weightiness [1]. The use of concrete and rubber scraps in structural concrete, according to Xie J, is a sustainable way to reduce environmental degradation brought on by solid waste and the depletion of natural resources [2]. According to ORTOLAN, extending a structure's service life was crucial for civil construction, both economically and in terms of user safety. One of the most prevalent issues was corrosion of steel bars, especially in areas with high chloride levels [3]. Faris studied the properties of geopolymer concrete by mixing fly ash with an alkaline activator in a sodium hydroxide and sodium silicate solution. Steel wool fibers were used to geopolymer concrete as reinforcement at varying weight percentages [4]. The purpose of Boukhalkhal S H was to compare the static and dynamic inelastic responses of rigid and semi-rigid connections of steel structures with steel to concrete columns constructed in seismically active areas to open-section columns. He discussed the benefits of flexural steel frames over those with open-section columns as well as the nonlinear dynamic response of these frames when constructed in seismically active areas [5]. According to academics, concrete is a crucial component of building and has to be thoroughly studied. In order to make the life of the building longer and save the cost, scholars are looking for better alternative materials.

The discrete element method is mainly used in the field of mechanical engineering, which can simulate the process of interaction and movement between spherical particles or various non-spherical particles and different mechanical parts. Nam J's powder filling simulation using the discrete element method found that there was a computational time limitation caused by the number and size of particles, and his new packing model can pack the data. It was found that the simulation time can be reduced by 400% using the new infill model [6]. Lv Y found that rockfall disasters often pose a significant threat to transportation infrastructure, passing vehicles and pedestrians. Therefore, it is very necessary to conduct in-depth research on the impact force of rockfall [7]. Canonne C L studied the problem of testing the structured properties of discrete distributions. Specifically, he developed a general algorithm for this problem that was suitable for a wide range of "shape-constrained" properties and is computationally efficient [8]. Yan B's goal was to use parallel computing on supercomputers to study the mechanical response of massive particle files by scanning simulations using discrete components of complex shapes ranging from thousands to millions of particles [9]. Scholars have found that discrete element method can effectively simulate things, especially in buildings, simulation calculation can greatly reduce people's workload and improve work efficiency. However, scholars have not established relevant simulation models in detail.

3. Simulation Calculation of Composite Beam Based on Discrete Element Method

Cast-in-place The use of composite structural columns, steel and concrete composite floors, etc., can address these drawbacks and have positive technical and financial effects. Concrete multi-layer frame structures and floor slabs require full scaffolding and full paving formwork. The composite structure has quickly advanced in engineering construction due to its benefits of saving steel, increasing material utilisation, lowering cost, providing strong seismic performance, and being simple to construct. Although composite structural research and use in China began much later, it has progressed quickly. Currently, some of them have been gathered into rules and some of them have been compiled into norms, which has helped to advance the development of composite structures in my nation. With the energy development of economy and society and the continuous acceleration of urbanization, people have put forward higher requirements for housing, transportation and energy use [10]. In recent years, accidents caused by low-quality building materials are shown in Figure 1.

As shown in Figure 1: These large-scale projects provide impetus for the development of the national economy, and at the same time occupy an important position in safe production and life. Due to the long construction time, complex structure, huge cost and long life cycle of these projects, it is

particularly important to ensure the safety of the structure during service. Once a safety accident occurs, it would threaten people's life and property safety, and have a negative impact on society. However, in the entire life cycle of engineering structures, various factors would inevitably cause damage, which may accumulate and affect the stiffness, strength and stability of the structure. If a certain degree of damage occurs, the safety, applicability and durability of the structure would be greatly reduced, and even the damage of the structure would lead to accidents.



Figure 1 Collapse accident

The form of steel and concrete single-sided composite beam is shown in Figure 2:

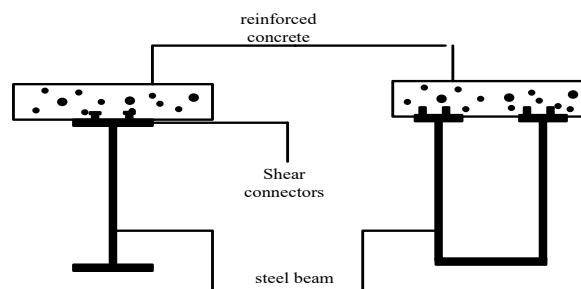


Figure 2 Steel and concrete single-sided composite beam

As shown in Figure 2: This is an early and widely used composite beam section form. The wings can be precast concrete slabs or cast on site. Compared with reinforced concrete beams, CB can speed up the construction progress and save the formwork process. Compared with steel beams, CB can significantly improve the stiffness and stability of beams, and have the advantages of large stiffness and small deflection.

3.1 Elastic Analysis of Steel-concrete Composite Section

In the elastic analysis, the rules of converting sections of material mechanics are used, one material is used as the main material, and the combined section formed by the two materials is converted into the section of one material by using the elastic modulus ratio. The composite beam section has obvious shear lag effect under the action of positive bending moment, and the corresponding normal stress at the steel main beam web is larger. The normal stress away from the web of the steel main girder is small, and the same negative bending moment area has obvious negative shear lag effect. When simplifying the calculation, it is considered that the normal stress is uniformly distributed within the effective width of the concrete slab.

After the composite section is converted into a section with steel as the main material by the principle of equal stiffness, the geometric properties of the section can be calculated by applying material mechanics, and then the strength and stiffness can be analyzed.

In the calculation, it is assumed that the contribution of the concrete support to the section stiffness is not calculated, and the steel is used as the main material to convert the area of the concrete slab into the area of the steel. The calculation Formula for the conversion area is Formula 1:

$$I'_I = I_0 + A_0 d_c^2 \quad (1)$$

The centroid position of the converted section is Formula 2

$$b = \frac{A_s b_s + A_c b_c / n}{A_s + A_c / n} \quad (2)$$

The strain ε of the concrete slab during concrete creep consists of two parts: elastic strain ε_e and creep strain ε_c as Formula 3:

$$E_1 = \frac{\varepsilon_e}{\varepsilon_c + \varepsilon_e} = \frac{\varepsilon_e}{\varphi(t_\infty, \tau)\varepsilon_c + \varepsilon_e} \quad (3)$$

In order to facilitate the calculation, the creep coefficient $\varphi(t_\infty, \tau)\varepsilon_c$ of concrete is introduced, so there is Formula 4:

$$k = \frac{\varepsilon_e}{\varepsilon_c + \varepsilon_e} = \frac{\varepsilon_e}{\varphi(t_\infty, \tau)\varepsilon_c + \varepsilon_e} = \frac{1}{1 + \varphi(t_\infty, \tau)} \quad (4)$$

The main influences on the creep effect of concrete are the ordinary steel bars in the concrete slab, the structural gravity, the shrinkage of the concrete and the live load. Some scholars have stipulated the coefficient k . When considering the influence of structural gravity, k is taken as 0.4. When considering the influence of shrinkage effect, k is taken as 0.5.

According to the assumption of elastic analysis, the slip between the steel main beam and the concrete slab is not considered, and the stress of the composite section can be calculated by using the converted section according to the assumption of the plane section. The stress calculation Formula of the steel main beam is Formula 5:

$$\sigma_s = \frac{M_b}{I_I'} \quad (5)$$

The Formula for calculating the stress of the concrete slab is Formula 6:

$$\sigma_s = \frac{M_b}{nI_I'} \quad (6)$$

In the Formula: M represents the design value of the bending moment of the composite beam section under the action of external load; b represents the distance between the stress calculation point and the centroid point of the section.

The concrete slab in the negative moment zone of the continuous beam with a composite section is highly easy to break under tension, and the elastic analysis does not take this into account when calculating the composite section's flexural resistance. The sole aspect of the composite section created by regular steel bars and steel main beams in the concrete slab that are taken into consideration in this research is its flexural stiffness. Figure 3 illustrates the computation of the cross-section of the composite beam's negative bending moment area.

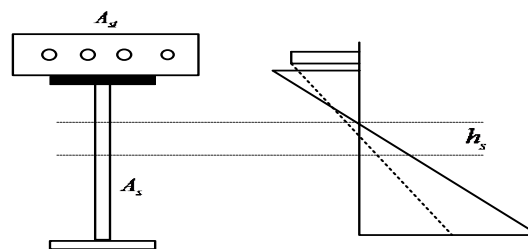


Figure 3 Section geometry and elastic stress distribution in the negative bending moment area of the composite section

Figure 3 illustrates how to compute the section geometry of the composite section's negative bending moment region. This study assumes that when the concrete slab is out of service, the contribution of the concrete section is not taken into account when computing the section's parameters. Formula 7 shows the distance between the centroid of the steel girder section and the neutral axis of the composite section.

$$h_e = \frac{A_{st}(h_s - h_{s1} + h_{st})}{A_s + A_{st}} \quad (7)$$

In the Formula: A_{st} represents the area of the tensile reinforcement within the effective width of the concrete; A_s represents the cross-sectional area of the steel main beam; h_{st} represents the distance from the bar centroid to the upper flange of the steel main beam. h_{s1} represents the distance from the bar centroid to the lower flange of the steel main girder; h_s represents the height of the steel girder section; the distance of the composite section is Formula 8:

$$b_s = h_{st} + h_e \quad (8)$$

Therefore, the bending moment of inertia of the composite section formed by the steel bar and the steel main beam in the negative bending moment area can be obtained as Formula 9:

$$I_2' = I_s = A_s b_s^2 + A_{sb} b_{st}^2 \quad (9)$$

In the calculation process, the contribution of the concrete in the negative moment area to the stiffness of the section is not taken into account, and the composite section is formed by ordinary steel bars and steel main beams. When calculating the effect of long-term load effects, the effect of concrete shrinkage and creep is not taken into account. Using the calculation of the bending-resistant beam of the mechanics of materials, the stress of the steel main beam is obtained as Formula 10:

$$\sigma_s = \frac{Mb}{I_2'} \quad (10)$$

The stress in the concrete section is Formula 11:

$$\sigma_c = \frac{Mb}{nI_2'} \quad (11)$$

In the Formula: M represents the design value of bending moment at the composite beam section under the action of external load; b represents the distance from the calculation point to the centroid of the converted section of the composite section. If the calculated maximum value of the stress σ_s of the steel main beam or the stress σ_c of the concrete slab reaches the design value of the elastic strength of the material, it is considered that the composite section has reached its elastic bearing capacity limit state. It is considered that the internal force acting on the composite section at this time reaches its ultimate elastic bearing capacity.

3.2 Simulation Calculation Based on Discrete Element Method

Using the discrete element approach, the functioning of steel-concrete CB is simulated and examined. The simulation results are then compared in order to develop discrete models and validate the steel-concrete CB' dependability. Typically, there are four ways to build the model. Particles are used in this research to build the discrete element model. In Figure 4, the established model is displayed.

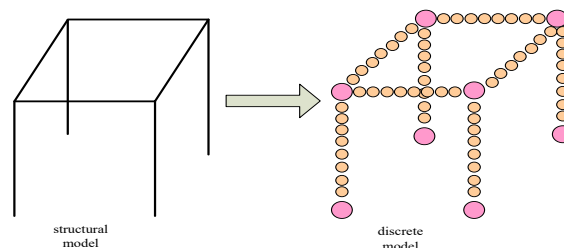


Figure 4 Discrete Element Simulation Model

Steel-concrete CB are similar to ordinary concrete with different parameters such as flexibility modulus and peak voltage. Therefore, the steel-concrete composite beam model replaces the ordinary concrete structure model, but the relevant parameters are adjusted accordingly. The concrete constitutive model adopts the modified model. The model considers the concrete tensile strength and linear tensile softening, and changes the stress-strain full curve by the constraint increase factor to consider the constraining effect of stirrups or section steel on the core concrete. The compression skeleton curve consists of three segments, and the mathematical expression is Formula 12:

$$\sigma_c = Kf'_c \left[2 \left(\frac{\varepsilon_c}{\varepsilon_0} \right) - \left(\frac{\varepsilon_c}{\varepsilon_0} \right)^2 \right] \quad (12)$$

Under the restraint of stirrups or section steel, the strength of steel and concrete CB has been greatly improved, and the ductility has also been improved. In order to accurately simulate the hysteretic behavior of concrete, according to the different restraint strengths, the concrete section of the beam-column with reinforced concrete is divided into three parts: unrestrained, general restraint and strong restraint. The three parts of concrete constitutive use different parameters respectively. The part from the outer surface of the stirrup to the outer edge of the member is unconstrained concrete, the part between the steel flanges is strongly constrained concrete, and the rest is general constrained concrete, as shown in Figure 5:

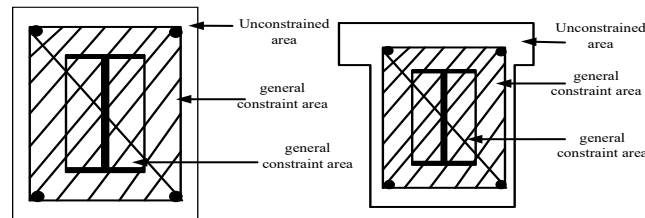


Figure 5 Schematic diagram of beam cross-section division

As shown in Figure 5: The transfer relationship between the cubic force under free concrete pressure and the equilibrium force under pressure is equal to Formula 13:

$$f_c^R = 0.76 f_{cu}^R \left(\frac{r}{2400} \right) \left(1 + \frac{R}{-89.338 R^2} \right) \quad (13)$$

In the Formula, R is the statistical regression coefficient, which is taken as 0.99. The peak strain of unconstrained concrete is Formula 14:

$$B(r) = r^2 - r \quad (14)$$

r is the apparent density of concrete, and $B(r)$ is the regression statistical parameter. For general restrained concrete, the increase coefficient K of the strength of the concrete by the restraint strength of stirrups can be calculated according to Formula 14. For strongly restrained concrete, the strength of concrete can be significantly improved and its deformation performance can be improved.

Intrinsic damping mainly comes from the internal friction of structural materials, connectors and non-structural components. Damping also affects the calculation method. If the damping is not selected properly, the calculation may not converge, and the result may be completely invalid. Among them, the damping matrix of Rayleigh damping satisfies the orthogonal condition of mode shape, its structure is reasonable, reliable, simple and convenient to use, and it is widely used in structural dynamic analysis.

Rayleigh damping is shown as in Formula 15:

$$[C] = a_0 [M] + a_1 [K] \quad (15)$$

The value of the initial stiffness matrix can be calculated from the initial elastic modulus of the material and the geometry of the member according to the following Formulas:

$$K = \begin{bmatrix} EA/L & 0 & 0 \\ 0 & 12EI/L^3 & -6EI/L^2 \\ 0 & -6EI/L^2 & 4EI/L \end{bmatrix} \quad (16)$$

$$EA = E_c A_c + E_a A_a \quad (17)$$

4. Simulation of Steel and Concrete CB

4.1 Experiment on Influence of Thickness of Steel and Concrete Composite Beam Bottom Plate

The experimental object selected in this paper is a bridge with a total length of 251m. The main girder adopts steel-concrete composite girder, and the cross section adopts the form of double steel box girder. The concrete bridge deck is made of C50 concrete, and the steel girder is made of Q345 steel. The bridge is modeled by discrete element method.

The model's computation outcomes match those of the traditional continuous beam, demonstrating the model's correctness and allowing for further study. By changing the steel beam's dimensions, this article would compare the structural impact under the original design conditions. Analysis is done to determine how the dimensions of the steel beam effect the displacement of the steel beam within the continuous steel-concrete composite beam as well as the stress on the bottom plate of the steel beam. The influence law of various parameter modifications on the steel-concrete composite continuous beam is obtained in order to understandably explain the stress characteristics of the steel-concrete composite continuous beam.

In this paper, the influence of different thicknesses of the bottom plate of steel beams on the mechanical properties is analyzed. For the bottom plate t , four thicknesses of 26mm (initial value, that is, the original design value), 30mm, 34mm, and 38mm are taken respectively, and the finite element model is calculated in this case. Figure 6 summarizes the effects of the thickness variation of the steel beam base plate on the mechanical performance of the steel-concrete composite continuous beam by analyzing and studying the change law of stress and deflection at the base plate at each characteristic point of the steel beam.

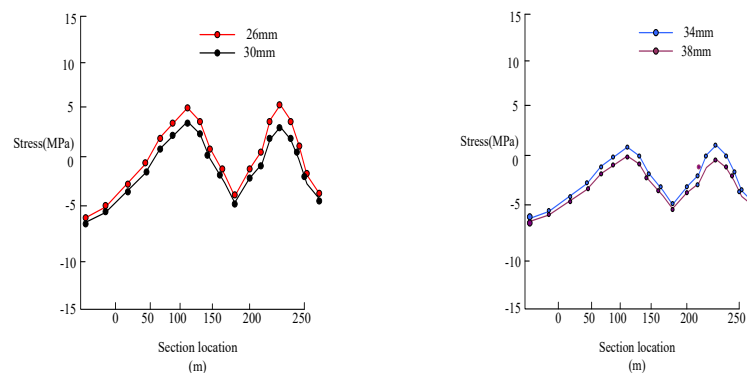


Figure 6 Base plate stress diagram of steel beams with different base plate thicknesses

Figure 6 shows that some parts of the steel carrier base plate are under voltage, while areas near the inflection point are under pressure. Regardless of pressure or thrust, the voltage value of the steel carrier bottom plate decreases with increasing plate thickness. It is beneficial to encourage the steel carrier by increasing the thickness of the substrate. The center valve is where the printed state of the substrate reaches its highest value. Importantly, the increased floor thickness below the steel carrier reduces floor pressure in the center of the shaft.

The variation law of stress and deflection of the characteristic point of the steel beam bottom plate is shown in Table 1.

The fluctuation law of the shift value conforms to the voltage values shown in Table 1. The mechanical properties and handling capacity of the steel-concrete composite beam are improved by collapsing the bottom plate of the steel carrier, thereby minimizing the flow of the carrier. According to

the variation law of voltage and displacement, it is assumed that increasing the thickness of the lower steel carrier plate within the specified range can effectively reduce the throughput voltage and throughput of the carrier. It can improve the mechanical properties to a certain extent.

Table 1 Displacement values of each characteristic point of the steel beam when the thickness t of the bottom plate of the steel beam is different (unit: mm)

thickness	starting point support	First span 1/4 position	1st span 1/2 position	1st span 3/4 position
26(mm)	0.00	55.66	6.19	-63.03
30(mm)	0.00	53.95	6.00	-61.06
34(mm)	0.00	53.30	5.82	-60.31
38(mm)	0.00	51.56	5.63	-58.31

4.2 Influence of Web Height of Steel and Concrete CB

The change law of mechanical properties of steel-concrete CB when the height of steel changes is studied. During the calculation and analysis, the changes in the height h of the steel support were -6 cm, -3 cm, 0 cm and 3 cm. The variation law of the voltage and flow rate on the base plate at each characteristic point of the steel carrier is studied, and the influence of the variation of the position height on the mechanical properties of the steel-concrete composite beam is summarized. Tables 2 and 3 show the variation of voltage and flow at the baseplate characteristics:

Table 2 The stress value of each characteristic point of the bottom plate of the steel beam when the height h of the steel beam is different (unit: MPa)

thickness	starting point support	First span 1/4 position	1st span 1/2 position	1st span 3/4 position
-6(cm)	0.00	66.28	7.38	-76.49
-3(cm)	0.00	58.79	6.53	-67.66
0(cm)	0.00	54.66	6.19	-63.03
3(cm)	0.00	51.66	5.75	-59.58

Table 3 Displacement values of each characteristic point of the steel beam when the web height h of the steel beam is different (unit: mm)

thickness	starting point support	First span 1/4 position	1st span 1/2 position	1st span 3/4 position
-6(cm)	0.00	-76.01	-39.11	22.70
-3(cm)	0.00	-62.45	-33.00	19.01
0(cm)	0.00	-49.99	-25.59	14.59
3(cm)	0.00	-45.36	-21.39	11.57

The base plate of the steel beam is compressed near the fulcrum, as shown in Tables 2 and 3, while the base plate is tensioned in other locations. The stress value of the steel beam bottom plate tends to decrease as the height of the steel beam web rises. This is caused by the steel beam web's increased height, which enhances the section's bending stiffness. It is evident that increasing the steel beam's height helps to lower the stress on the structure.

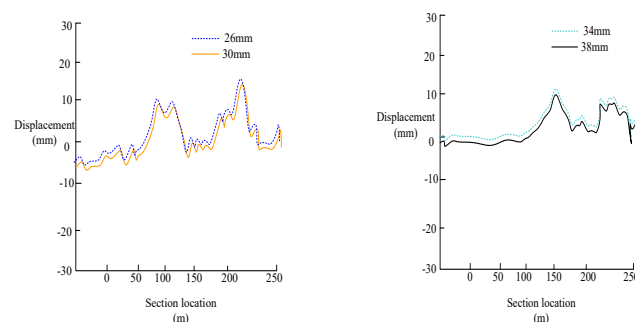


Figure 7 Displacement of steel beam with different web height h

The displacement of the steel beam when the web height h is different is shown in Figure 7:

Figure 7 illustrates how increasing the web height of the steel beam increases its bending stiffness

and, thus, increases its ability to resist deflection during construction. According to the variation law of stress and displacement, it is thought that increasing the web height of steel beams within a specified range would somewhat enhance the mechanical and service performance of continuous steel-concrete composite beams. Clearly, the steel beam's web height has a considerable impact on the section's bending stiffness. However, when the web height of the steel beam rises, the section height of the continuous steel-concrete composite also rises.

4.3 Influence of Web Thickness of Steel and Concrete CB

The experiment investigates the thickness change of steel beam webs using the variation law of mechanical characteristics of continuous steel-concrete composite beams. The calculation and analysis are carried out when the thickness of the steel beam web is 16 mm, 18 mm, 20 mm, and 22 mm, respectively. Similar to this, the variation law of stress and deflection at the base plate is explored at each characteristic point of the steel beam, and the impact of the change in web thickness on the mechanical performance of the continuous steel-concrete composite beam is outlined. The variation law for the stress and deflection at the unique point of the bottom plate of the steel beam is shown in Figure 8.

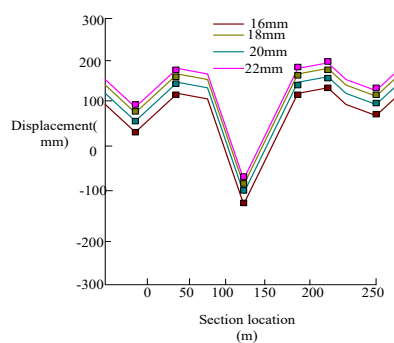
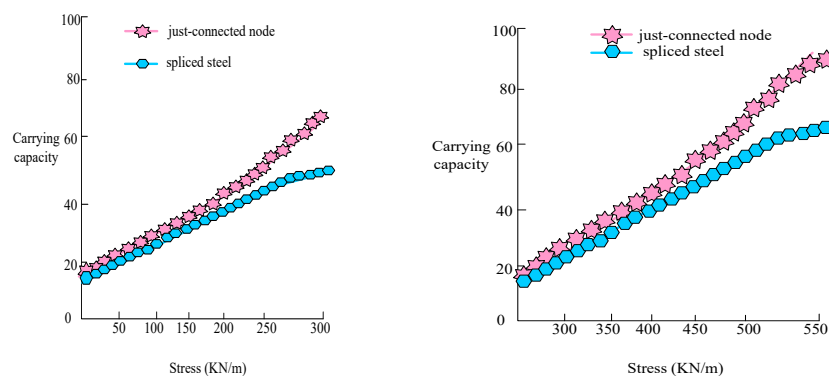


Figure 8 Displacement of steel beam with different web thickness

As seen in Figure 8, increasing the steel beam web's thickness can lessen structural deflection, and the law is consistent with how changing the web height affects steel beam displacement. The web thickness may be more effective in improving the section's shear resistance because its contribution to the section's bending moment of inertia is quite minimal. With the growth of the web, the proportion of self-weight increases is very obvious, so increasing the thickness of the web has no effect on improving the mechanical properties of the steel-concrete composite continuous beam.

4.4 Comparison of Carrying Capacity

The maximum normal stress appears at the lower flange plate of the steel main girder in the left span as the load increases until the friction force is overcome, as shown in Figure 9. The spliced joints also exhibit rotational characteristics as the load increases, and the normal stress of the section is redistributed.



(a) Bearing capacity of spliced steel main beams (b) Steel bearing capacity of rigid joints

Figure 9 Comparison of bearing capacity of different steel main beams

According to Figure 9: Figure 9(a) shows that as the load is increased, the steel and concrete

composite beam that is connected to the steel main beam initially enters the stress yield condition. The steel-concrete composite beam at the rigid junction has a larger bearing capacity, accounting for up to 90%, as can be shown in Figure 9(b).

On the basis of the aforementioned, it can be stated that raising the bottom plate and web plate thickness can enhance structural performance while having a negligible impact on web plate height. In engineering practice, the optimization of structure size should be treated with caution, so as to avoid unnecessary waste. In the project, the accuracy of the structural dimensions must be ensured. The reduction of the structural size has a great influence on the bearing capacity, which is a permanent weakening. During the construction process, the requirements of the design documents must be strictly followed.

5. Conclusion

Steel and concrete CB make up for the defects of reinforced concrete beams, make full use of the tensile properties of steel and the compressive properties of concrete, and improve the spanning capacity of CB. Compared with the composite beam of steel and concrete, the simply supported beam has more advantages in cross-domain performance and service performance. The discrete element method simulation model is chosen in this research to carry out intelligent simulation calculation of the interface connection between steel and concrete CB and grasp its bearing capacity and characteristics. Utilizing the discrete element method, the structure of CB made of steel and concrete is examined. In the experiment, it was found that three conditions independently increased the thickness of the bottom plate of the steel beam, the thickness of the web of the steel beam, and the height of the web. The stress and deflection of the steel-concrete composite continuous beam section have improved to varying degrees, which is favourable for the steel-concrete composite continuous beam's bearing capacity and service performance. It follows that CB built of steel and concrete clearly have very high bearing capacities and degrees of stability. Although the experiment still has some defects, building should always be flawless.

References

- [1] Karthik S, Rao P, Awoyera P O. *Strength properties of bamboo and steel reinforced concrete containing manufactured sand and mineral admixtures*[J]. *Journal of King Saud University - Engineering Sciences*, 2017, 29(4):400-406.
- [2] Xie J , Li J , Lu Z , Li Z, Fang C, Huang L. *Combination effects of rubber and silica fume on the fracture behaviour of steel-fibre recycled aggregate concrete*[J]. *Construction & Building Materials*, 2019, 203(APR.10):164-173.
- [3] ORTOLAN, Vinicius, de, Kayser. *Comparative assessment of corrosion of concrete reinforced with unprotected steel and hot-dip galvanized steel*. [J]. *Revista de la construcción*, 2017, 16(2):238-248.
- [4] Faris, Meor, Ahmad. *Performance of Steel Wool Fiber Reinforced Geopolymer Concrete*. [J]. *AIP Conference Proceedings*, 2017, 1885(1):1-5.
- [5] Boukhalkhal S H , Ihaddoudene A , Neves L , Madi W. *Dynamic behavior of concrete filled steel tubular columns*[J]. *International Journal of Structural Integrity*, 2019, 10(2):244-264.
- [6] Nam J , Lyu J , Park J . *Particle generation to minimize the computing time of the discrete element method for particle packing simulation*[J]. *Journal of Mechanical Science and Technology*, 2022, 36(7):3561-3571.
- [7] Lv Y , Li H , Zhu X , Song NN, Zheng Z. *Discrete element method simulation of random Voronoi grain-based models*[J]. *Cluster Computing*, 2017, 20(1):335-345.
- [8] Canonne C L , Diakonikolas I , Gouleakis T , Rubinfeld R. *Testing Shape Restrictions of Discrete Distributions*[J]. *Theory of computing systems*, 2018, 62(1):4-62.
- [9] Yan B , Regueiro R . *Large-scale dynamic and static simulations of complex-shaped granular materials using parallel three-dimensional discrete element method (DEM) on DoD supercomputers*[J]. *Engineering Computations*, 2018, 35(2):1049-1084.
- [10] Fukuda D , Mohammadnejad M , Liu H . *Development of a 3D Hybrid Finite-Discrete Element Simulator Based on GPGPU-Parallelized Computation for Modelling Rock Fracturing Under Quasi-Static and Dynamic Loading Conditions*[J]. *Rock Mechanics and Rock Engineering*, 2020, 53(3):1079-1112.